first converted to total path lengths. The theoretical curve of Lindhard *et al.*[4] has been computed for $k=0.16$, a value that is appropriate to all the data under consideration. It is seen that both the present results and those of Bryde *et al.*[10] are in very good agreement with the theoretical curve over the entire energy range covered in these studies. This agreement substantiates the belief that Lindhard's theory may be validly applied to the analysis of thick-target recoil data up to moderately high recoil energies.

The data of Van Lint *et al.*[9] lie well above the theoretical curve. Although these results do not quite overlap in recoil energy with the present data, it appears that the two sets of results are mutually inconsistent. This is probably related to the fact that it is difficult to obtain an accurate estimate of the recoil energy from a (γ,n) reaction induced by bremsstrahlung.

The low-energy data may also be compared with the Monte Carlo calculation of Oen *et al.*[5] of the ranges of low-energy atoms in solids. Their results for the total path length of Cu atoms slowing down in Cu have been transformed to $\rho-\epsilon$ coordinates and are shown by the dashed line in Fig. 2. This curve, based on Bohr's value for the screening length, predicts range values that are significantly larger than the present results. The calculated curve can be brought into better agreement with experiment by increasing the screening length, as suggested by Oen *et al.*[5]

ACKNOWLEDGMENTS

The cooperation of Dr. C. P. Baker and the operating crew of the Brookhaven 60-in. cyclotron is appreciated. The chemical yield determinations were ably performed by the Brookhaven Chemistry Department Analytical Group.

PHYSICAL REVIEW VOLUME 135, NUMBER 4A 17 AUGUST 1964

Effective g Factor of Electrons and Holes in Bismuth

G. E. Smith, G. A. Baraff, and J. M. Rowell
Bell Telephone Laboratories, Murray Hill, New Jersey
(Received 11 March 1964)

Shubnikov–de Haas type oscillations have been studied in bismuth in magnetic fields up to 88 kG. Oscillations are observed which have been attributed to the hole band in bismuth. A machine calculation of the density of states and of the Fermi level as a function of magnetic field is used to fit the data. The calculation is based on the nonparabolic (two-band) model of the electron band, and includes the possibility of spin splitting for both electrons and holes. It correctly predicts the observed change in Fermi energy with magnetic field. We find that the hole Landau levels are indeed split by spin. The spin splitting is almost twice the Landau level spacing along the trigonal axis and is extremely small perpendicular to the trigonal axis. Spin splitting is also observed for electrons. We find that the spin splitting is about one-third the orbital splitting in the heaviest mass direction and about 10% larger than the orbital splitting in the light mass direction. Our observations imply that there are important states both above and below the hole band. This is in direct contradiction to the Abrikosov and Falkovskii model which considers only one set of states (either above the hole band or below) with which the hole band interacts.

I. INTRODUCTION

It is well known that the transverse energy of electron or hole states in a magnetic field will be quantized, the allowed energies being called Landau levels and the spacing between levels being proportional to the field strength H. Since the electron has a spin degree of freedom, each Landau level has a twofold degeneracy arising from spin. Associated with the spin is a magnetic moment whose energy E_m in the magnetic field is also proportional to the field strength. This energy is often written $E_m=\frac{1}{2}g\beta_0 H$, β_0 being the Bohr magneton and g being denoted the effective g factor. This energy may add to or subtract from the energy of the Landau level, thus splitting each level into a pair of levels. The density of states at the Fermi level in a magnetic field is determined to a large extent by the spacing and splitting of the Landau levels. This paper reports on oscillations in the magnetoresistance of bismuth which result from a change in scattering time as the density of states at the Fermi level is changed by the magnetic field. Previously unobserved oscillations are seen at high field which are attributed to spin splitting of the hole band. With the magnetic field parallel to the binary axis, oscillations from the heavy electron mass are observed and the spin splitting is found to be different than the Landau spacing.

The magnitude of the g factor depends on details of the band structure. For free electrons, $g=2$. The g factor for electrons in bismuth was calculated by Cohen and Blount[1] to be $g=2m_0/m_c$, m_c being the cyclotron effective mass. This value of g factor yields a spin

[1] M. H. Cohen and E. I. Blount, Phil. Mag. **5**, 115 (1960).

splitting equal to the Landau level spacing and has been generally verified by the phase of observed de Haas–van Alphen oscillations[2] and by infrared magnetoreflection experiments.[3] A 10% departure from $g=2m_0/m_c$ has been reported[4] for the light electron mass with the magnetic field parallel to the binary axis. de Haas–van Alphen oscillations attributed to holes have been observed at low magnetic field by Brandt[5] but no spin splitting was reported.

A recent model of the bismuth band structure proposed by Abrikosov and Falkovskii[6] has been used by Falkovskii[7] to calculate the energy levels of the holes in a magnetic field parallel to the trigonal axis. This model leads to a spin splitting equal to the Landau level spacing so that separate periods for spin and orbital splitting cannot be observed. Our observations are in definite disagreement with this model and indicate that there are important states both above and below the hole band which are neglected in the Abrikosov-Falkovskii model.

II. THEORY

A. Band Structure of Bismuth

The model of the band structure of bismuth which we use to interpret the data consists of a set of three equivalent electron ellipsoids and a single hole ellipsoid. In one of the electron ellipsoids, the energy E is related to the momentum $\mathbf{p}$ in the absence of a magnetic field by

$$E[1+(E/E_G)]=\mathbf{p}\cdot\boldsymbol{\alpha}\cdot\mathbf{p}/2m_0, \tag{1}$$

where E_G is the energy gap to the next lower band and $\mathbf{m}^*=\boldsymbol{\alpha}^{-1}$ is the effective mass tensor in units of the free electron mass m_0. The inverse effective mass tensor $\boldsymbol{\alpha}$ is of the form

$$\boldsymbol{\alpha}=\begin{bmatrix}\alpha_{11} & 0 & 0\\ 0 & \alpha_{22} & \alpha_{23}\\ 0 & \alpha_{23} & \alpha_{33}\end{bmatrix}, \tag{2}$$

where 1, 2, and 3 refer to the binary, bisectrix, and trigonal axes, respectively. The other two electron ellipsoids are obtained by rotations of $\pm 120°$ about the trigonal axis. The energy momentum relationship (1) is that predicted by the two-band model[8] in which the presence of a nearby band at an energy E_G below alters the energy-momentum dependence from the more usual quadratic dependence obtained formally by letting E_G in Eq. (1) become infinite. It should be pointed out that the two-band model which leads to Eq. (1) is an approximation in which the influence of all bands other than the two separated by E_G are neglected. The validity of this approximation will be discussed in Sec. V.

For the holes, the energy momentum relationship in the absence of a magnetic field is taken to be

$$E_0-E=\frac{1}{2m_0}[(p_1^2+p_2^2)/M_1+(p_3^2/M_3)], \tag{3}$$

which corresponds to an inverse mass tensor

$$\boldsymbol{\alpha}^h=\begin{bmatrix}1/M_1 & 0 & 0\\ 0 & 1/M_1 & 0\\ 0 & 0 & 1/M_3\end{bmatrix} \tag{4}$$

for the holes. E_0 is the energy of the top of the hole band relative to the bottom of the electron band.

The spatial density of carriers in each ellipsoid is determined by the Fermi energy E_F and is proportional to the volume of $\mathbf{p}$ space bounded by the surface $E=E_F$. The Fermi energy is found by adjusting E_F to give equality between the spatial density of holes and that of electrons.

B. Density of States and Fermi Level in the Presence of a Magnetic Field

In the presence of a magnetic field in the z direction, the eigenstates of the electron can be labeled by quantum numbers n, p_y, p_z and $s=\pm 1$. The energy E instead of being dependent on p_x, p_y and p_z, now becomes

$$E(1+E/E_G)=(n+\tfrac{1}{2})\hbar\omega_c+p_z^2/2m_z\pm\tfrac{1}{2}g\beta_0 H, \tag{5}$$

where ω_c is the cyclotron frequency

$$\omega_c=eH/m_c c,$$

and where the longitudinal and the cyclotron masses m_z and m_c are

$$m_z=\mathbf{h}\cdot\mathbf{m}^*\cdot\mathbf{h}, \tag{6a}$$

$$m_c=[\det\mathbf{m}^*/m_z]^{1/2}. \tag{6b}$$

The vector $\mathbf{h}$ is a unit vector in the direction of the magnetic field H. The effective g factor may be defined in terms of a spin mass[1] tensor $\mathbf{m}_s$ by

$$g^2=4m_0^2\mathbf{h}\cdot\mathbf{m}_s\cdot\mathbf{h}/\det\mathbf{m}_s. \tag{7}$$

The spin and effective masses defined here are those taken at the bottom of band (m_b). Conventional cyclotron masses refer to masses $m(E_F)$ taken at the Fermi energy. These masses are related to ours by

$$m(E_F)=[1+(2E_F/E_G)]m_b. \tag{8}$$

Equality of spin splitting and the Landau spacing

[2] J. S. Dhillon and D. Shoenberg, Phil. Trans. Roy Soc. London **A248**, 1 (1955).
[3] R. N. Brown, J. G. Mavroides, and B. Lax, Phys. Rev. **129**, 2055 (1963).
[4] J. E. Kunzler, F. S. L. Hsu, and W. S. Boyle, Phys. Rev. **128**, 1084 (1962).
[5] N. B. Brandt and M. V. Razumeenko, Zh. Eksperim. i Teor. Fiz. **39**, 276 (1960) [English transl.: Soviet Phys.—JETP **12**, 198 (1961)].
[6] A. A. Abrikosov and L. A. Falkovskii, Zh. Eksperim. i Teor. Fiz. **43**, 1089 (1962) [English transl.: Soviet Phys.—JETP **16**, 769 (1963)].
[7] L. A. Falkovskii, Zh. Eksperim. i Teor. Fiz. **44**, 1935 (1963) [English transl.: Soviet Phys.—JETP **17**, 1302 (1963)].
[8] P. A. Wolff (unpublished). B. Lax, J. G. Mavroides, H. J. Zeiger, and R. J. Keyes, Phys. Rev. Letters **5**, 241 (1960).

implies $m_s=m^*$, as is predicted by the two-band model. These equations apply to each of the three equivalent electron ellipsoids. For the single hole ellipsoid where there is no evidence for a two-band picture, the expression (E_0-E) replaces the left-hand side of (5) and, as in (3), the tensor $\boldsymbol{\alpha}^h$ is used in (6). Similarly, an effective spin mass, m_{sh}, may be defined for the holes by Eq. (7).

From the electron energy (5) and the spatial dependence of the wave function (but not the energy) on p_y,[9] one can obtain the spatial density of states whose energy is less than E_F.

$$N_i^e(E_F)=(2^{3/2}eH/h^2c)(m_z)^{1/2}\times\sum_{n,s}\{E_F^*-E(n,s)\}^{1/2}, \quad (9)$$

where

$$E_F^*=E_F(1+E_F/E_G), \quad (10)$$

and

$$E(n,s)=(n+\tfrac{1}{2})\hbar\omega_c+\tfrac{1}{2}s\beta_0 gH. \quad (11)$$

The sum is over those values of n and of $s=\pm1$ such that the radicand is positive. The derivative of this expression with respect to the Fermi energy gives the density of states at the Fermi surface:

$$\mathfrak{N}_i^e(E_F)=(2^{3/2}eH/h^2c)(m_z)^{1/2}\sum_{n,s}\tfrac{1}{2}(1+2E_F/E_G)\times\{E_F^*-E(n,s)\}^{-1/2}. \quad (12)$$

These expressions apply of course to each of the electron ellipsoids; for each ellipsoid, the value of m_c, m_z, and g will be different because each of the three ellipsoids has a different orientation.

For the single hole ellipsoid, the number of states whose energy is above E_F is

$$N_h(E_F)=(2^{3/2}eH/h^2c)(m_z)^{1/2}\times\sum_{n,s}\{(E_0-E_F)-E(n,s)\}^{1/2}, \quad (13)$$

and the density of states, the (absolute value of the) derivative of this expression with respect to E_F is

$$\mathfrak{N}_h(E_F)=(2^{3/2}eH/h^2c)(m_z)^{1/2}\times\sum_{n,s}\tfrac{1}{2}\{(E_0-E_F-E(n,s)\}^{-1/2}. \quad (14)$$

The sum again goes over values of n and s for which the radicand is positive. Charge neutrality requires that

$$\sum_{i=1}^{3}N_i^e(E_F)=N_h(E_F) \quad (15)$$

and this equation determines the Fermi energy.

The solution of (15) for E_F is markedly affected by the magnetic field; the Fermi level itself shows oscillatory behavior. The shift in Fermi level is one of the reasons that the de Haas–van Alphen oscillations are not strictly periodic in reciprocal field. It must be included in the analysis of any high-field experiments.

Having determined the Fermi energy, one can evaluate the number of carriers in each pocket and the corresponding density of states. Maxima in the density of states (corresponding to minima in the resistance) can then be plotted as a function of field strength and orientation. It is these plots which are fitted to the data by adjusting the parameters of the model.

III. EXPERIMENTAL METHOD

This experiment originated in an attempt to find de Haas–van Alphen type oscillations in the capacitance of a structure consisting of a flat surface of single-crystal bismuth covered with Formvar and then plated with an aluminum layer. The aluminum layer was formed by evaporating a 30-mil-diam spot and contact to the spot was made with silver paste. Impedance measurements were made with a 100 kc/sec bridge. Although there were no observable changes in capacitance, the method proved to be a convenient way of measuring the oscillations in the series resistance of the 30-mil point contact on the bismuth slab. To obtain continuous measurements as a function of magnetic field, the null meter of the bridge was disconnected and a dc microvoltmeter put in its place. Balancing the bridge at zero magnetic field and plotting the unbalance of the bridge as a function of magnetic field on a recorder exhibited the oscillations in the resistance. Examples of such plots are shown in Figs. 1 and 2. The magnetic field was provided by an 88 kG solenoid and the sample was rotated with respect to the field direction by a gear arrangement in the Dewar.

To obtain the large relaxation times needed for the observation of these oscillations, high-purity zone-leveled bismuth was used and the measurements were made at 1.4°K. Single crystals were grown by the pulling technique and cut into crystallographically oriented slabs by an acid string saw. Electrical contact was made

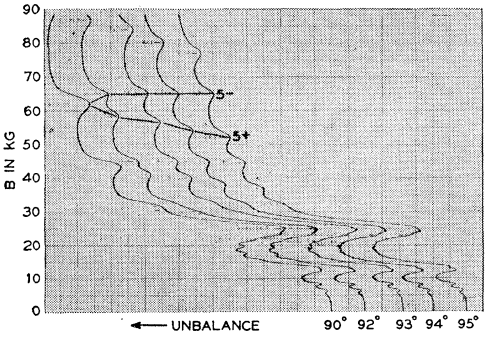

FIG. 1. Impedance bridge unbalance versus magnetic field strength for field direction in the $y-z$ plane. The y axis is at 90°. Spin splitting of the hole oscillations appear as the field is rotated away from the y axis. Quantum numbers for two of these levels $(n=5,\ s=\pm1)$ have been indicated on this figure.

[9] A. H. Kahn and P. R. Frederikse, in *Solid State Physics*, edited by F. Seitz and D. Turnbull (Academic Press Inc., New York, 1959), Vol. 9.

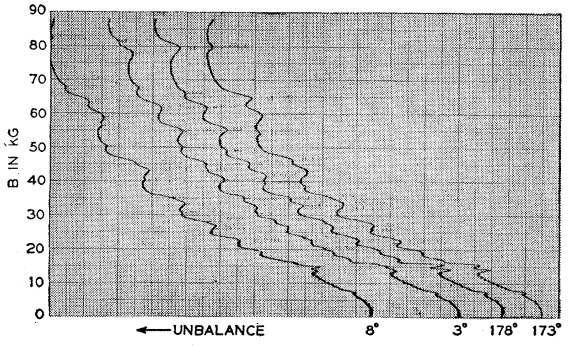

FIG. 2. Impedance bridge unbalance versus magnetic field strength for field direction in the $x-z$ plane.

to one face of the slab by soldering. The opposite face was acid lapped and electropolished. A thin insulating layer was deposited on this face either by dipping in a Formvar solution or by the Langmuir technique using stearic acid or a similar film. Capacitors were formed by evaporating an array of 30-mil-diam spots of aluminum onto the insulator through a mask. Contact to these dots was made using silver paste and aluminum foil leads. Typically, the capacitance of the structure was 10^{-9} F and the series resistance of the leads and contact was about 100 Ω. The resistance of the bismuth increased from essentially zero at zero field to about 50 Ω at 88 kG. The change in capacitance was less than one part in 10^4.

IV. RESULTS

The locations of peaks in the density of states as a function of magnetic field were obtained by noting minima in the resistance. These points correspond to minima in relaxation time resulting from maxima in the density of states and at low fields along principal crystallographic orientations, agree with peaks seen by other methods, e.g., de Haas–van Alphen effect,[2] magnetothermal oscillations,[4] etc. The usual method of plotting periods in $\Delta(1/H)$ as a function of crystallographic direction is not applicable to the high-field data presented here since the peaks are no longer periodic in $1/H$. Instead, the peak position in $1/H$ is plotted as a function of crystallographic direction, giving rise to a series of curves corresponding to individual Landau levels. Such plots are presented in Figs. 3 and 4.

The calculated plots were obtained using the theory presented in Sec. III. The calculations were carried out using an IBM-7090 computer. Effective masses for the electrons and holes are essentially those obtained from hybrid resonance experiments[10] and are presented in Table I. The masses labeled "at Fermi level" are taken at the zero-field Fermi level [see Eq. (8)]. The energy gap for the electron band, $E_G=15.3$ meV, was obtained from magnetoreflection experiments[3] and a band overlap of $E_0=38.5$ meV was chosen to fit our data. The resulting Fermi energy at zero magnetic field is $E_F=27.6$ meV which agrees with $E_F=25\pm5$ meV obtained from magnetoreflection experiments. The total number of electrons is calculated from the above parameters to be $N_e=2.75\times10^{17}/\text{cm}^3$ at zero field. Cyclotron and spin masses along principal axes are presented in Table II and are evaluated at the zero-field Fermi level.

[10] G. E. Smith, L. C. Hebel, and S. J. Buchsbaum, Phys. Rev. 129, 154 (1963).

TABLE I. Orbital and spin effective mass components for electrons and holes in bismuth. The Fermi energy E_F and number of carriers are calculated from these masses, the energy gap E_G and the band overlap E_0.

Electrons	m_{11}	m_{22}	m_{33}	m_{23}
Orbital				
at bottom of band	0.00113	0.26	0.00443	−0.0195
at Fermi energy	0.00521	1.20	0.0204	−0.090
Spin mass				
at bottom of band	0.00101	2.12	0.0109	−0.13
at Fermi energy	0.00466	9.77	0.0502	−0.60

Holes	$M_1=M_2$	M_3
Orbital mass	0.064	0.69
Spin mass	0.033	200
$E_G=15.3$ meV	$E_0=38.5$ meV	
$E_F=27.6$ meV	$N_e=N_h=2.75\times10^{17}/\text{cm}^3$	

The hole and electron spin masses were chosen to fit our data and are presented in Table I. The major problem in fitting the data was the assignment of quantum numbers (n and s) to the levels. This corresponds to choosing a proper shape for the g tensor relative to the effective mass tensor and many possibilities were tried. The general procedure was to choose a labeling scheme and then to vary the parameters to see if a fit could be achieved.

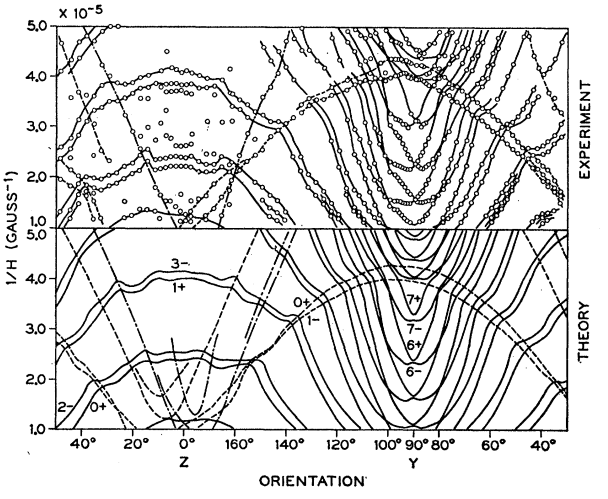

FIG. 3. Peak positions of individual quantum levels as a function of $1/H$ and field direction for rotation of H in the $y-z$ plane. A few levels have been labeled with their quantum numbers (the 6+ level means $n=6$, $s=+1$). The solid lines are hole levels and the dashed lines are electron levels.

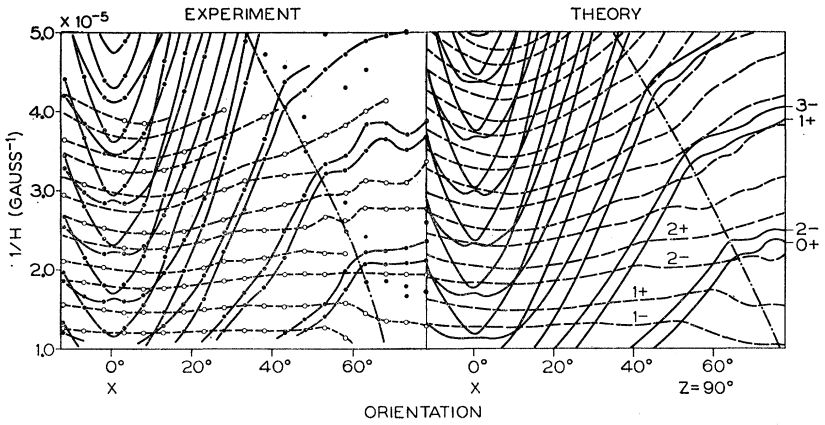

FIG. 4. Peak positions of individual quantum levels as a function of $1/H$ and field direction for rotation of H in the $x-z$ plane. The open points are the small amplitude electron oscillations in Fig. 2 and the solid points are hole oscillations.

In Figs. 3 and 4 one sees that the hole oscillations could be resolved for all orientations. The heaviest electron periods can be seen clearly about the binary and bisectrix axes but as the magnetic field is rotated towards the trigonal axis, oscillations from the other two-electron ellipsoids appear and the resolution of the peaks is not sufficient to make unambiguous identifications. Because of this, neither theoretical plots or experimental lines were drawn in the figures except for the few shown at high fields in Fig. 3.

Experimental plots of quantum number n versus $1/H$ are shown in Fig. 5, for H along the bisectrix axis, and in Fig. 6, for H along the binary axis. The hole oscillations depart from periodicity in $1/H$ at high magnetic field in a way which indicates that the Fermi energy is dropping monotonically with increasing field. This drop in Fermi energy comes about, we believe, because the electrons have a lowest quantum level slightly below the band minimum (i.e., we believe that $g>2m_0/m_c$ for at least one of the three-electron ellipsoids when the field is in this orientation). This single level will move down slightly in energy as the field is increased, while all the other levels move up in energy. The other levels eventually cross the Fermi surface and play no active role, leaving this one level beneath the Fermi surface.

TABLE II. Orbital and spin effective masses for electrons and holes in bismuth taken along principal crystallographic axes. These masses are evaluated at the zero-field Fermi energy, $E_F=27.6$ meV.

H‖Trigonal axis	Orbital	Spin
Electrons	0.065	0.11
Holes	0.064	0.033
H‖Binary axis		
Electrons	0.128	0.36
	0.0097	0.0091
Holes	0.21	1.5
H‖Bisectrix axis		
Electrons	0.0084	0.0079
	0.0168	0.0158
Holes	0.21	1.5

As the field increases, so too does the number of electrons which can be fit into this single Landau level increase [see Eq. (13)] and this increase tends to pull the Fermi level down. Plots of the variation of Fermi level obtained from the calculation are shown for the field along three principal axes in Figs. 7, 8, and 9. This variation in Fermi level also changes the number of carriers in the various electron and hole pockets and this variation for H along the binary axis is shown in Fig. 10. It should be made clear that Figs. 5 through 10 are calculated curves using parameters necessary to fit the data and are made plausible by the observed variation of hole period with field.

V. SUMMARY AND CONCLUSIONS

One major new result from these measurements is the observation of a new set of periods which we at-

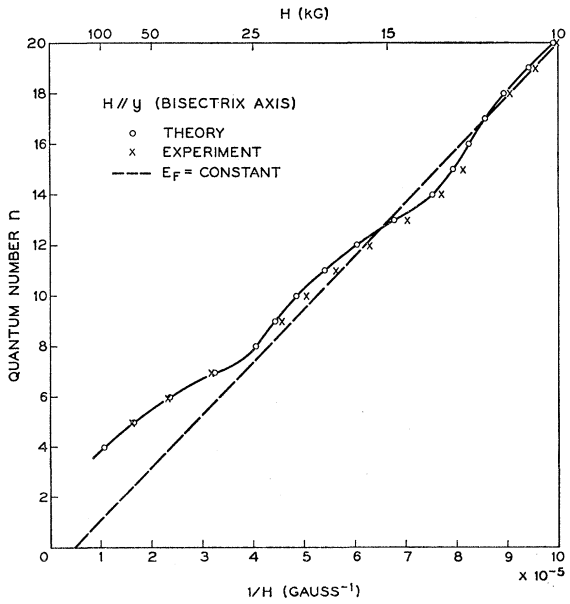

FIG. 5. Quantum number n versus $1/H$ for hole oscillations with H along the bisectrix axis. The solid line connects the theoretical points.

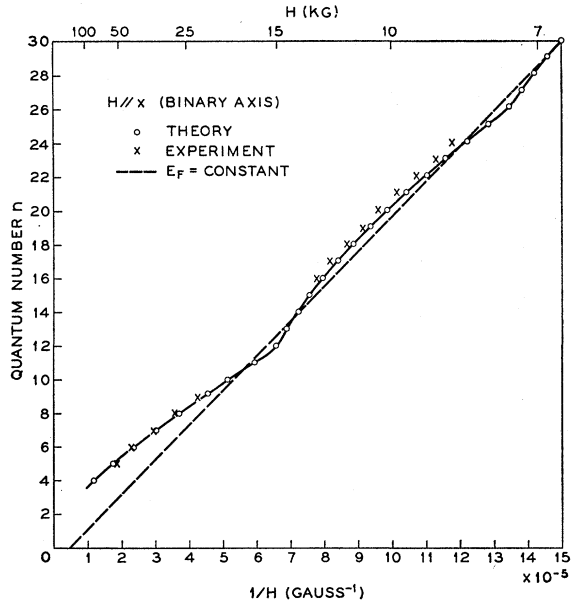

FIG. 6. Quantum number n versus $1/H$ for hole oscillations with H along the binary axis. The solid line connects the theoretical points.

tribute to spin splitting of the hole band. It would be possible to fit the data by postulating a band contributing a third set of carriers but two coincidences would then have to occur: (1) that the new carriers should give rise to Landau levels whose spacing, in a magnetic field *anywhere* in the plane perpendicular to the trigonal axis, is the same as the spacing of the hole levels and; (2) that the amplitudes of the oscillations arising from Landau levels in the new band should be equal to the amplitude of oscillations arising from the hole Landau levels. (See Figs. 1 and 2.) These coincidences imply great similarity in the shapes of the new band and the hole band. This seems to us to be unlikely.

The effective g factor for the hole band is quite obviously dependent on the orientation of the magnetic field. There is some latitude in the choice of this dependence.

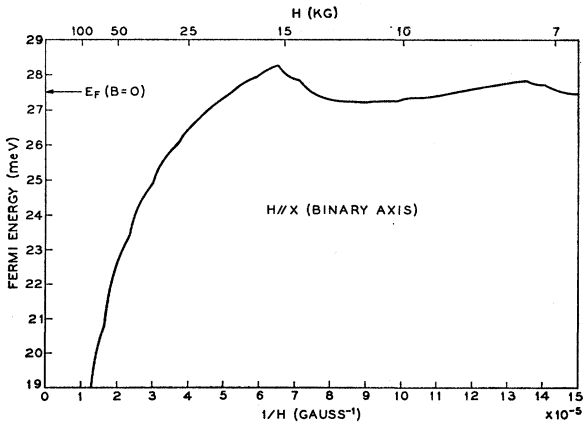

FIG. 7. Fermi level versus $1/H$ parallel to the binary axis.

The results presented here follow from a choice of g in the form given by Eq. (7) with the tensor m_s chosen to give the largest value of g along the trigonal axis. (A polar plot of g would be cigar shaped.) By relabeling the levels, it should be possible to fit the data with a g factor which is smallest along the trigonal axis (pancake shape). Variation of the parameters in Eq. (7) to give a pancake shape yields a best fit inferior to that of the cigar-shaped g factor. Hence, if the g factor is to be pancake shaped, it will have to be at least quartic in its dependence on the direction cosines of the field. The same can be said for the possibility that the g factor be positive along one major axis and negative along the other. The cigar-shaped g factor has one other feature which strongly recommends it, a feature which is related to the symmetry properties of the electronic states. It turns out that Bloch waves whose k vector lies along the trigonal axis (where the holes are thought to occur) can be of only two basic symmetry types,

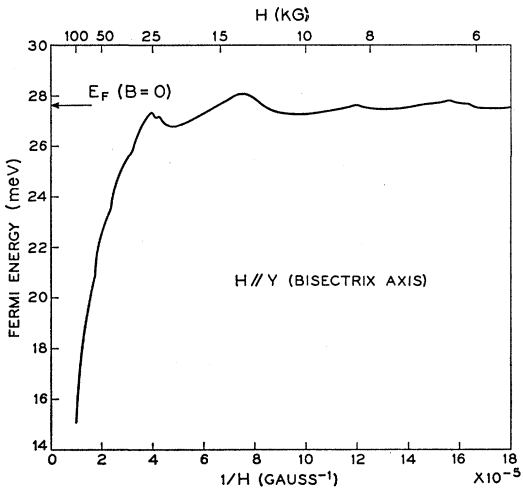

FIG. 8. Fermi level versus $1/H$ for H parallel to the bisectrix axis.

designated by Mase[11] as A_4+A_5 and A_6 (either with or without primes). For one of these types, A_4+A_5, the transverse spin splitting vanishes automatically,[12] regardless of the existence or energy of other states whose k is also along the trigonal axis. That is, for this type of state, the g factor is cigar shaped to the extreme. Our choice of a cigar-shaped g factor leads to a g factor sufficiently elongated for us to identify the hole band as of the $A_4'+A_5'$ symmetry type. Mase's tight binding calculation (see Fig. 3 of Ref. 11) does, in fact predict the hole band as being of this symmetry type.

The magnitude of the hole g factor was chosen to be $g\cong 1$ for the magnetic field perpendicular to the trigonal axis. The resolution of the peaks is such, however, that

[11] S. Mase, J. Phys. Soc. Japan **13**, 434 (1958).
[12] E. I. Blount (private communication).

it can only be certain that $g<2$. With the field parallel to the trigonal axis, the spin splitting is almost twice the orbital splitting. Although the two-band model assumed for the electron band does not permit the spin splitting to differ from the orbital splitting, the larger effective masses found for the hole band indicate that for them a two-band model is not valid, i.e., there are other bands nearby in energy which interact with the hole band. The presence of other nearby bands admits the possibility of a spin splitting larger than the orbital splitting provided that there are important bands both above and below the hole band.[12]

A small (less than 10%) splitting of the electron ellipsoids having the lightest cyclotron masses was observed about the binary and bisectrix axes. This could be interpreted as a spin splitting either slightly greater than or slightly less than the orbital splitting. With a spin splitting less than the orbital splitting, the drop in Fermi level along the bisectrix axis was not sufficient to explain the observed change in the period of the hole oscillations, so the larger splitting was chosen. Also, in the angular variation in the $y-z$ plane, there appears to be a crossing of the 0+ and 1− electron levels at about 145° as required by this scheme (see Fig. 3).

Oscillations with the field in the $x-z$ plane were observed and identified as the heavy cyclotron mass electron ellipsoid split by spin. These are the small bumps seen in Fig. 2 and plotted as open points in Fig. 4. The spin splitting could be larger or smaller than the orbital splitting and the case of larger splitting was ruled out

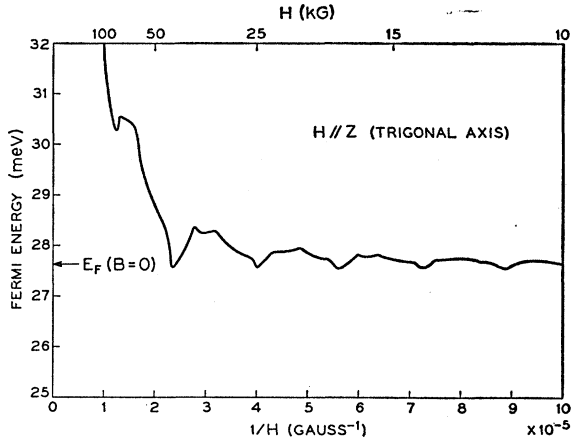

FIG. 9. Fermi level versus $1/H$ for H parallel to the trigonal axis.

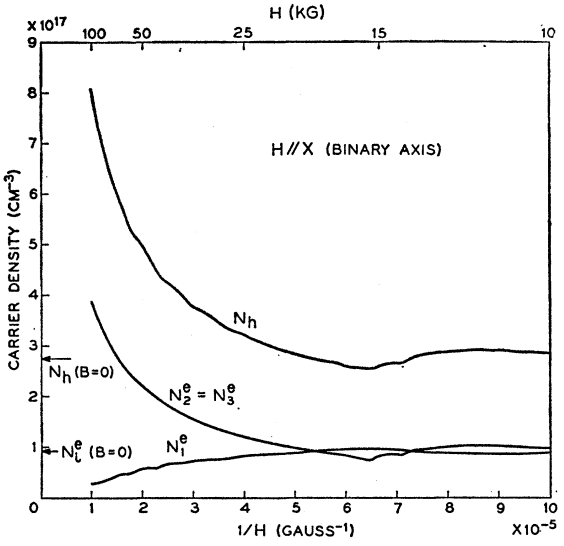

FIG. 10. Carrier density versus $1/H$ for H parallel to the binary axis. The symbol $N_1{}^e$ refers to the number of carriers in the electron ellipsoid with the heaviest cyclotron mass.

because some of the levels would have to merge together as the field was rotated towards the trigonal axis and this was not observed. For the other alternative, the choice between a spin splitting one third or two thirds of the Landau spacing had to be made. To do this, the cyclotron mass of the heavy electron obtained from microwave resonance[13] was assumed correct and numerically, the one third splitting gave a much better fit.

The fact that in certain directions the spin splitting is greater than the orbital splitting for electrons implies deviations from the two-band model and the need to consider additional bands.

One curiosity in the data is the apparent tripling of both electron and hole oscillations at high fields for orientations about 50° and 130° in Fig. 3. We have no good explanation for this phenomenon.

ACKNOWLEDGMENTS

We wish to thank Dr. E. I. Blount and Dr. Y. Yafet for stimulating discussions concerning the hole spin splitting.

[13] L. C. Hebel (to be published) has interpreted the resonance at 3.2 kG in Fig. 9 of Ref. 10 as cyclotron resonance of the heavy electron rather than spin resonance as was previously assumed. The resonance is a result of a slightly nonlocal current-field relation and is not a tilted orbit cyclotron resonance.